PROCEEDINGS OF SCIENCE

Nucleosynthesis in jet-induced supernovae

Nozomu Tominaga[*†]
Department of Physics, Faculty of Science and Engineering, Konan University
8-9-1 Okamoto, Kobe, Hyogo 658-8501, Japan
E-mail: tominaga@konan-u.ac.jp

The first metal enrichment in the universe was made by supernova (SN) explosions of population III stars and the results are recorded in abundance patterns of extremely metal-poor (EMP) stars. Meanwhile, it has been found that gamma-ray bursts with relativistic jets are associated with highly-energetic SNe (hypernovae) and observations of SNe in recent days also smoke out that SNe are universally aspherical. Thus, I present hydrodynamical and nucleosynthetic properties of the jet-induced explosion of a population III star with a two-dimensional special relativistic hydrodynamical code. In the jet-induced SNe, Fe-peak products are ejected along the jet axis, while unprocessed materials fall onto a central remnant along the equatorial plane. This coexistence accounts for the abundance patterns of the EMP stars. Also, the jet-induced explosion realizes the high-entropy environment that enhances [(Sc, Ti, V, Cr, Co, Zn)/Fe]. The enhancements of [Sc/Fe] and [Ti/Fe] improve agreements with the abundance patterns of the EMP stars. Furthermore, I point out that the evidence of jet-induced SN is found in a Si-deficient metal-poor star HE 1424-0241 with high [Mg/Si] ($= 1.4$) and normal [Mg/Fe] ($= 0.4$). While the peculiar abundance pattern is difficult to be reproduced by previous SN models, it can be reproduced only by the angle-delimited yield of the jet-induced SN if the interaction between the SN ejecta and interstellar medium induces a weak mixing of the abundances.

11th Symposium on Nuclei in the Cosmos, NIC XI
July 19-23, 2010
Heidelberg, Germany

[*]Speaker.
[†]The appointed researcher of the Institute for the Physics and Mathematics of the Universe.

PoS(NIC XI)163

1. Introduction

In the early universe, the enrichment by a single supernova (SN) can dominate the preexisting metal contents (e.g., [1]). The Pop III SN shock compresses the SN ejecta consisting of heavy elements, e.g., O, Mg, Si, and Fe, and the circumstellar materials consisting of H and He. The abundance pattern of the enriched gas reflects nucleosynthesis in the SN and the second-generation stars will be formed from the enriched gases. Thus the abundances of the second generation stars preserve the information of nucleosynthesis in Pop III SNe [2].

Present-day photometric and spectroscopic observations indicate that gamma-ray bursts (GRBs) and SNe are aspherical explosions with jet(s) (e.g., [3, 4, 5]). Such aspherical SN explosions are also suggested in the early universe by the abundance patterns of extremely metal-poor (EMP) stars with [Fe/H] < -3.[1] The C-enhanced type of the EMP stars have been well explained by the faint SNe [6, 7], except for their large Co/Fe and Zn/Fe ratios (e.g., [8]). The enhancement of Co and Zn in low metallicity stars requires explosive nucleosynthesis under high entropy. In a *spherical* model, a high entropy explosion corresponds to a high energy explosion that inevitably synthesizes a large amount of ^{56}Ni. Thus, it was suggested that some faint SNe are associated with a narrow jet within which a high entropy region is confined [9].

In this paper, I present hydrodynamical and nucleosynthetic models of the jet-induced explosions of a 40 $M_\odot$ star and show that only an angular-delimited yield of a jet-induced SN explosion can account for an abundance pattern of a peculiar Si-deficient EMP star. Furthermore, I compare the jet-induced explosion with the spherical SN model applied the mixing-fallback model [10] and connect properties of the jet-induced explosion to the mixing-fallback model.

2. Models

I investigate a jet-induced SN explosion of a Pop III $40M_\odot$ star with a two-dimensional relativistic Eulerian hydrodynamic and nucleosynthesis calculation (see [11, 12] for the model detail). Because the explosion mechanism of GRB-associated SNe is still under debate, I do not consider how the jet is launched but deal the jet parametrically with the following five parameters: energy deposition rate ($\dot{E}_{\rm dep}$), total deposited energy ($E_{\rm dep}$), initial half angle of the jets ($\theta_{\rm jet}$), initial Lorentz factor ($\Gamma_{\rm jet}$), and the ratio of thermal to total deposited energies ($f_{\rm th}$). The jet is injected from the inner boundary at an enclosed mass M_0 corresponding to a radius R_0. In this paper, I show two models; (A) a model with $\dot{E}_{\rm dep,51} = \dot{E}_{\rm dep}/(10^{51}\,{\rm ergs\ s^{-1}}) = 120$ and $M_0 = 1.4M_\odot$ ($R_0 = 900$ km) and (B) a model with $\dot{E}_{\rm dep,51} = 120$ and $M_0 = 2.3M_\odot$ ($R_0 = 2700$ km). The other parameters are same for each model; $E_{\rm dep} = 1.5 \times 10^{52}$ ergs, $\theta_{\rm jet} = 15^\circ$, $\Gamma_{\rm jet} = 100$ and $f_{\rm th} = 10^{-3}$. The mass of jets is $M_{\rm jet} \sim 8 \times 10^{-5} M_\odot$.

3. Results

The hydrodynamical calculations are followed until the homologously expanding structure is reached ($v \propto r$). Then, the ejected mass elements are identified from whether their radial velocities

[1] Here [A/B] $= \log_{10}(N_{\rm A}/N_{\rm B}) - \log_{10}(N_{\rm A}/N_{\rm B})_\odot$, where the subscript $\odot$ refers to the solar value and $N_{\rm A}$ and $N_{\rm B}$ are the abundances of elements A and B, respectively.

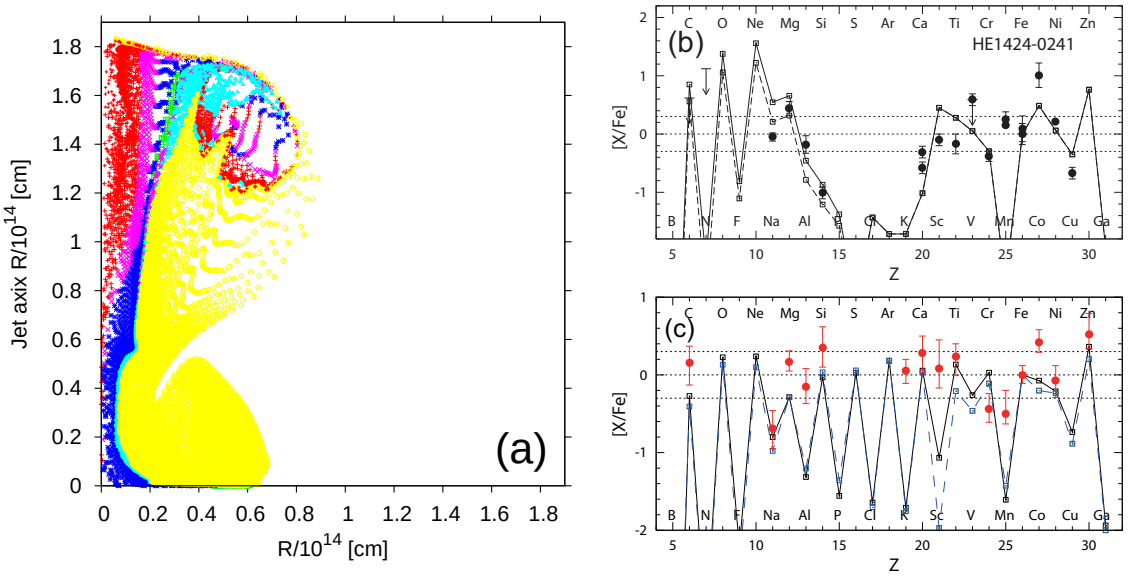

Figure 1: (a) Positions of the mass elements at $t = 10^5$ s for model A. Symbols of the marks represents the abundance of the mass element (H: *circle*, He: *triangles*, O+C: *squares*, O+Mg: *stars*, Si: *crosses*, and Fe: *pluses*). Size of the marks represents the origin of the mass element (the jet: *dots*, and the shocked stellar mantle: *filled circles*). (b) Comparison between the abundance pattern of HE 1424–0241 (*filled circles*) and the angle-delimited yields of model A for $30° \leq \theta < 40°$ (*solid line*) and $30° \leq \theta < 35°$ (*dashed line*). (c) Comparison of the abundance patterns of model B (*solid line*), the EMP stars (*filled circles*, [13]), and the mixing-fallback models with $M_{\rm cut}({\rm ini}) = 2.3 M_\odot$, $M_{\rm mix}({\rm out}) = 10.3 M_\odot$ and $f = 0.27$ (*dashed line*).

exceed the escape velocities at their positions. Figures 1a shows the abundance distribution at $t = 10^5$ s for model A. I classify the mass elements by their abundances as follows: (1) Fe with $X(^{56}{\rm Ni}) > 0.04$, (2) Si with $X(^{28}{\rm Si}) > 0.08$, (3) O+Mg with $X(^{16}{\rm O}) > 0.6$ and $X(^{24}{\rm Mg}) > 0.01$, (4) O+C with $X(^{16}{\rm O}) > 0.6$ and $X(^{12}{\rm C}) > 0.1$, (5) He with $X(^{4}{\rm He}) > 0.7$, and (6) H with $X(^{1}{\rm H}) > 0.3$. If a mass element satisfies two or more conditions, the mass element is classified into the class with the smallest number.

3.1 Abundance patterns of the metal-poor stars

A very peculiar, Si-deficient, metal-poor star HE 1424–0241 was observed [14]. Its abundance pattern with high [Mg/Si] (~ 1.4) and normal [Mg/Fe] (~ 0.4) is difficult to be reproduced by previous SN models. This is because $\log\{[X({\rm Mg})/X({\rm Si})]/[X({\rm Mg})/X({\rm Si})]_\odot\} \lesssim 1.6$ is realized in the O+Mg layer at the presupernova stage (e.g., [15, 9]). Thus, in order to reproduce the abundance pattern of HE 1424–0241, the SN yield is required to include explosively-synthesized Fe but not explosively-synthesized Si.

The angle-delimited yield may possibly explain the high [Mg/Si] and normal [Mg/Fe] (Fig. 1b). Figure 1b shows that the yields integrated over $30° \leq \theta < 40°$ and $30° \leq \theta < 35°$ of model A reproduce the abundance pattern of HE 1424–0241. The yield consist of Mg in the inner region and Fe in the outer region (Fig. 1a). Although there are some elements to be improved, the elusive feature of HE 1424–0241 could be explained by taking into account the angular dependence of the yield. The high [Mg/Si] and normal [Mg/Fe] can be realized with an appropriate integration range

if the Fe mass elements penetrate the stellar mantle (i.e., the duration of the jet injection is long) and if the O+Mg mass elements are ejected in all directions (i.e., $\dot{E}_{\rm dep}$ is high).

3.2 Comparison with the spherical supernova model

The calculations of the jet-induced explosions show that the ejection of the inner matter is compatible with the fallback of the outer matter. This is consistent with the two-dimensional illustration of the mixing-fallback model (Fig. 12b in [16]).

I clarify the relation between the mixing-fallback model and the jet-induced explosion model by comparing the yields. The mixing-fallback model has three parameters; initial mass cut [$M_{\rm cut}({\rm ini})$], outer boundary of the mixing region [$M_{\rm mix}({\rm out})$], and a fraction of matter ejected from the mixing region (f). The remnant mass is written as $M_{\rm rem} = M_{\rm cut}({\rm ini}) + (1-f)[M_{\rm mix}({\rm out}) - M_{\rm cut}({\rm ini})]$. The three parameters would relate to the hydrodynamical properties of the jet-induced explosion models, e.g., the inner boundary (M_0), the outer edge of the accreted region ($M_{\rm acc,out}$), and the width between the edge of the accreted region and the jet axis.

The angle-integrated yield of model B is compared with the yields of the spherical SN model with $M_{\rm ms} = 40 M_\odot$ and $E_{\rm dep} = 3 \times 10^{52}$ ergs. The inner boundary, the outer edge of the accreted region, and the central remnant mass of model B are $M_0 = 2.3 M_\odot$, $M_{\rm acc,out} = 12.2 M_\odot$, and $M_{\rm rem} = 8.1 M_\odot$. For the spherical SN model, the explosion energy is deposited instantaneously as a thermal bomb and I set $M_{\rm cut}({\rm ini})$ to be the same as M_0 [i.e., $M_{\rm cut}({\rm ini}) = 2.3 M_\odot$] and apply $M_{\rm mix}({\rm out}) = 10.3 M_\odot$ and $f = 0.27$. f is the fraction of the solid angle of the Si-burning region (hereafter the fraction is written as $f_{\rm Si}$). $M_{\rm mix}({\rm out})$ is set to yield the same $M_{\rm rem}$ as model B. The angle-integrated abundance pattern of model B is roughly reproduced by the mixing-fallback model (Fig. 1c). Thus, I conclude that the jet-induced explosion is approximated by the mixing-fallback model reasonably. M_0, $f_{\rm Si}$, and $M_{\rm rem}$ in the jet-induced explosion model are represented by $M_{\rm cut}({\rm ini})$, f, and $M_{\rm rem}$ in the mixing-fallback model, respectively.

There are some elements showing differences, Sc, Ti, V, Cr, Co, and Zn. The enhancements of [Sc/Fe] and [Ti/Fe] improve agreements with the observations. The differences stem from the high-entropy explosion due to the concentration of the energy injection in the jet-induced explosion (e.g., [17]). Such thermodynamical features of the jet-induced explosion model cannot be reproduced by the mixing-fallback model exactly but a "low-density" modification might mimic the high-entropy environment (e.g., [9, 16]).

4. Conclusions and Discussion

I present the aspherical abundance distributions and investigate the angular dependence of the yield. The abundance distributions in the jet-induced SN ejecta could be examined by spatially-resolved observations of supernova remnants (e.g., [18]). The angle-delimited yield could reproduce the extremely peculiar abundance pattern of HE 1424–0241. However, the angle-delimited yields of model A have a large scatter that may be inconsistent with the relatively small scatter in the abundance ratios of the EMP stars. This implies that the angular dependence of the yield in most SNe is diluted by the strong mixing of the SN ejecta. The angle-delimited yield strongly depends on which mass elements are included into the integration. This would be determined by the abundance mixing in the SN ejecta [19] and by the region where the next-generation star takes in

the metal-enriched gas. To investigate this issue further, it is required to calculate three-dimensional evolution of the supernova remnant in the ISM.

The angle-integrated yield of the jet-induced explosion is well reproduced by a spherical SN model applied the mixing-fallback model. This confirms that the mixing-fallback model approximates the jet-induced explosion well and that the mixing and fallback in hypernovae assumed in the mixing-fallback model are actually achieved in aspherical explosions. The abundance ratios between elements synthesized in different regions (e.g., C, O, Mg, and Fe) depend on the hydrodynamical structure of the explosion, e.g., the fallback. Thus, such macroscopic properties of the jet-induced explosion are represented by the mixing-fallback model. In particular, M_0, $f_{\rm Si}$, and $M_{\rm rem}$ in the jet-induced explosion model are represented by $M_{\rm cut}({\rm ini})$, f, and $M_{\rm rem}$ in the mixing-fallback model, respectively. On the other hand, the ratios between the explosively-synthesized elements depend on the thermodynamical properties of the explosion. In particular, [Sc/Fe], [Ti/Fe], [V/Fe], [Cr/Fe], [Co/Fe] and [Zn/Fe] are enhanced by the high-entropy environment in the jet-induced explosion, thus showing differences from the mixing-fallback model. The enhancement of [Sc/Fe] and [Ti/Fe] improve the agreement with the observations.

References

[1] J. Audouze & J. Silk, J., *ApJ* **451** (1995) L49

[2] T. C. Beers & N. Christlieb, *ARA&A* **43** (2005) 531

[3] D. A. Frail, et al., *ApJ* **562** (2001) L55

[4] K. Maeda, et al., *ApJ* **565** (2002) 405

[5] K. Maeda, et al., *Science* **319** (2008) 1220

[6] H. Umeda & K. Nomoto, *Nature* **422** (2003) 871

[7] N. Iwamoto, H. Umeda, N. Tominaga, K. Nomoto, K. Maeda, *Science* **309** (2005) 451

[8] E. Depagne, et al., *A&A* **390** (2002) 187

[9] H. Umeda & K. Nomoto, *ApJ* **619** (2005) 427

[10] H. Umeda & K. Nomoto, *ApJ* **565** (2002) 385

[11] N. Tominaga, et al., *ApJ* **657** (2007) L77

[12] N. Tominaga, *ApJ* **690** (2009) 526

[13] R. Cayrel, et al., *A&A* **416** (2004) 1117

[14] J. G. Cohen, et al., *ApJ* **659** (2007) L161

[15] S. E. Woosley & T. A. Weaver, *ApJS* **101** (1995) 181

[16] N. Tominaga, H. Umeda, & K. Nomoto, *ApJ* **660** (2007) 516

[17] K. Maeda & K. Nomoto, *ApJ* **598** (2003) 1163

[18] U. Hwang, et al., *ApJ* **615** (2004) L117

[19] N. Nakasato & T. Shigeyama, *ApJ* **541** (2000) L59